19th Australasian Fluid Mechanics Conference
Melbourne, Australia
8-11 December 2014

Implicit Enthalpy Method for Modelling Laser Induced Melting and Solidification of Silicon

M.S. Ahmmed[1], M.Talei[2] and E.R.Hawkes[3]

[1]School of Mechanical and Manufacturing Engineering
The University of New South Wales, Sydney 2052, Australia

[2]Department of Mechanical Engineering
The University of Melbourne, Melbourne, Victoria 3010, Australia

[3]School of Mechanical and Manufacturing Engineering/ School of Photovoltaic and Renewable Energy Engineering
The University of New South Wales, Sydney 2052, Australia

Abstract

This paper presents a numerical study of laser induced melting and solidification of crystalline Silicon (Si) using an implicit enthalpy method. The simulations are performed using the open source C++ solver known as OpenFOAM [1]. The model considers temperature dependent thermo-physical and optical properties for Si. To verify the numerical model, its predictions are compared with the experimental results for a nanosecond pulsed laser annealing of Si with pulse duration of 30 ns and wavelength (λ) of 308 nm. An excellent agreement with the experimental results is observed for both the melting depth and the melting duration. In the second part of this study, the KrF excimer laser (λ = 248 nm) annealing of Si wafer widely used for production of solar cells is simulated. The effects of substrate heating on the melting duration, and re-crystallisation velocity are then investigated. Our results show that, for a given pulse duration, the maximum re-crystallisation velocity is almost independent of the laser power but decreases with the substrate heating.

Introduction

Laser annealing of Si has received a considerable attention in the solar cell manufacturing industry. This is due to the capability of the laser processing in modification of the structural defects [2] and doping of the Si solar cells [3]. The use of pulse laser beams in the nanosecond regime allows depositing a precise amount of energy in a short time into the surface region. Under suitable conditions, irradiation leads to the melting of the Si surface, and re-crystallisation from the bulk with a high melting front velocity. In the laser doping process, it is necessary to have a prolonged melting duration along with a slow re-crystallisation velocity [4]. A high re-crystallisation velocity, resulting from a rapid change in the temperature, generates defects within the solidified Si [2]. Additionally, a fast heating process combined with the limited thermal conductivity of Si creates a spatial temperature gradient not only at the surface but also in the deeper regions of the wafer. This temperature gradient enhances the formation of mechanical stress in the Si [2, 5]. To overcome these problems, longer pulse durations may be used. However, changing the pulse duration for a laser system is not a straightforward task [5]. The alternative to this method is the substrate heating of the wafer [4].

Numerous analytical and numerical techniques have been developed to solve laser induced melting and solidification of Si. Analytical models based on the Green's function [6-10] have been employed for this problem, but they are limited to the solid state regime. This is due to the strong non-linearity of the heat equation when melting occurs. The numerical models, based on the explicit [4,11-15] and the implicit [16-18] enthalpy formulations, are extensively used to overcome this problem. Although the explicit scheme is easy to implement, a special treatment of the time steps is required to ensure stability [15]. Most of the implicit enthalpy methods [16-18] assume that the phase change occurs over a range of temperature rather than at a single temperature. This assumption is not realistic in the case of Si melting [4].

In the present paper, a numerical model based on the implicit enthalpy method is developed to simulate the laser induced melting and solidification of Si. In contrast to the other implicit models [16-18], the phase change occurs in a single temperature in the present model. We simulated the process of nanosecond pulse laser induced melting and solidification of Si for the laser beam wavelength (λ) of 248 nm (pulse duration of 32 ns and 45ns), which is widely used for solar cells manufacturing [12,14,19]. A number of simulations are performed to shed light on the influence of substrate heating on the melting duration, re-crystallisation velocity and thermal gradients.

Mathematical Model

To obtain the temperature field and capture the propagation of melting front due to laser irradiation, the thermal conduction theory can be used [4]. The incident laser beam is assumed to be aligned perpendicular to the wafer surface, and has a Gaussian based temporal shape defined by the full width half maximum (FWHM). Figure 1 shows a schematic of the problem. An energy-based formulation of the heat conduction equation, taking into account the enthalpy of melting/solidification, may be written as [14-15],

$$\frac{dH}{dt} = \nabla(K\nabla T) + Q_l \,, \tag{1}$$

where, H is the total enthalpy, K is the thermal conductivity and Q_l is the laser heat source. The laser heat source may be expressed as [11,16-17],

$$Q_l = I_0(1-R)\alpha F(t)\exp(-\alpha y) \,, \tag{2}$$

where, I_0 is the laser power density, R is the reflection coefficient, α is the absorption coefficient and *F(t)* is the Gaussian temporal distribution function. The enthalpy in equation (1), consists of the sensible enthalpy and the latent heat of fusion when melting/solidification is considered. Therefore, the total enthalpy may be expressed as [14],

$$H = h + \gamma\rho L_f = \int_{T_{ref}}^{T} \rho C_p dT + \gamma\rho L_f \ , \quad (3)$$

where, h is the sensible enthalpy, ρ is the density, C_p is the specific heat capacity, L_f is the latent heat of fusion, T_{ref} is the reference temperature and γ is the liquid fraction. Substituting equation (3) into equation (1) leads to the following form of the energy equation,

$$\frac{d(\rho CpT)}{dt} = \nabla(K\nabla T) + Q_l - \rho L_f \frac{d\gamma}{dt} \ . \quad (4)$$

The liquid fraction in equation (4) is a Heaviside step function which may be written as,

$$\gamma = 1, T > T_M \ \text{ and } \ \gamma = 0, T < T_M \ , \quad (5)$$

where, T_M is the melting temperature. Obtaining the temperature field usually requires an iterative process between equations (4) and (5) which is referred to as the temperature based update method [20-21]. One of the major problems for this approach is that the numerical solution is prone to instability in the form of oscillations [21]. This is due to an extreme sensitivity of the phase fraction to small changes in temperature, which may leads to a mutually inconsistent γ and T fields [21]. To overcome these problems, we updated the liquid fraction based on the enthalpy in an iterative manner. Our developed method is similar to the method presented by Voller [20] and Shyy *et al.* [21]. The solution algorithm can be described as:

(a) The iterative process is started by setting $\gamma^0 = \gamma^{old}$ where, old is the old time step

(b) Equation (4) is solved to obtain the temperature field T^{m+1} where, m is the iteration level

(c) The liquid fraction γ^{m+1} is calculated based on the enthalpy field as,

$$h^{m+1} = \rho C_p T^{m+1} \ , \quad (6)$$

$$\gamma^{m+1} = \gamma^m + \omega\left(\frac{h^{m+1} - H_s}{H_l - H_s}\right) , \quad (7)$$

$$H_s = \rho C_p T_M \ , H_l = \rho C_p T_M + \rho L_f \ , \quad (8)$$

where, H_s is the solidus enthalpy, H_l is the liquidus enthalpy and ω is the relaxation factor

(d) The steps (b)-(c) are continued until the convergence is achieved. The following criteria is applied to every node at each step of this procedure

$$\gamma^{m+1} = 0 \quad if \quad \gamma^{m+1} < 0 \ \text{and} \quad (9)$$

$$\gamma^{m+1} = 1 \quad if \quad \gamma^{m+1} > 1 . \quad (10)$$

Numerical Methods

The introduced model was implemented into the open source computational fluid dynamics (CFD) software, OpenFOAM [1]. OpenFOAM is a Linux-based C++ framework providing the essential library for solving complex fluid flow phenomena involving heat transfer. Equation (4) is discretised using the control volume approach. A second-order accurate central differencing scheme is used for the spatial term and the Euler implicit method is used for the temporal discretisation. Since the thermal conductivity of Si is strongly temperature dependent, a careful treatment of the conduction term $\nabla(K\nabla T)$ is required. We therefore employed harmonic averaging [1] to calculate the heat flux across the face between two control volumes rather than using the arithmetic averaging. As a result, the energy conservation is guaranteed.

The initial and boundary conditions for the problem may be written as [4],

$$T(x, y, 0) = T_i \ , \quad (11)$$

$$-k\left.\frac{dT}{dx}\right|_{y=0} = -k\left.\frac{dT}{dy}\right|_{x=0} = 0 \ , \quad (12)$$

$$-k\left.\frac{dT}{dy}\right|_{y=L} = 0 \ , T(x, d, t) = T_i \ , \quad (13)$$

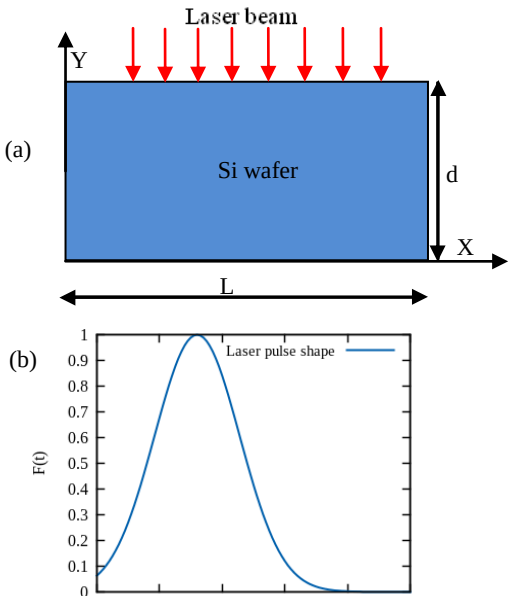

Figure 1. Schematic diagram for laser irradiated Si (a), and Gaussian beam (b).

where, T_i is the initial temperature, d is the thickness of the wafer and L is the length of the wafer.

The thermo-physical and optical properties of Si are obtained from the published experimental results [4,12-13,15].

Comparison with the Experimental Results

The numerical model is validated with the experimental results presented by Unamuno *et al.* [12] and Aziz *et al.* [13]. In these experiments, the melting depth in crystalline Si was determined by the transmission electron microscopy (TEM). The time resolved optical reflectivity measurements were performed to determine the onset and duration of the surface melting. To

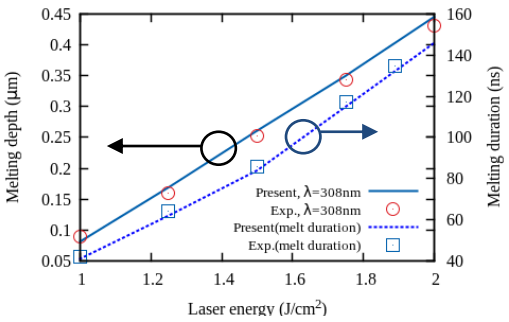

Figure 2. Comparison of the numerical and the experimental results presented by Unamuno *et al.* [12] and Aziz *et al.* [13] for the melting depth and the melting duration as a function of laser energy density (λ=308nm and FWHM = 30 ns).

compare with the experimental results, simulations have been carried out for λ=308 nm and FWHM=30 ns. Figure 2 shows a comparison between the numerical and experimental results for the melting depth and melting duration for λ=308 nm and FWHM=30 ns. As can be seen, there is an excellent agreement between the numerical and experimental results.

Results and Discussions

In the following section, simulations have been carried out for the wafer irradiated at the laser power of 1 J/cm^2 to 2 J/cm^2 with the pulse duration (i.e. FWHM) of 32 ns and 45 ns, and the substrate temperature of 300°C and 500°C for λ=248 nm. Figure 3 shows the maximum surface temperature as a function of time for a number of laser powers and pulse durations of 32 ns and 45ns. As expected, the temperature of the wafer increases with the increase of the laser energy density for both pulse durations. For a given laser power density, the surface temperature decreases as the laser pulse duration increases.

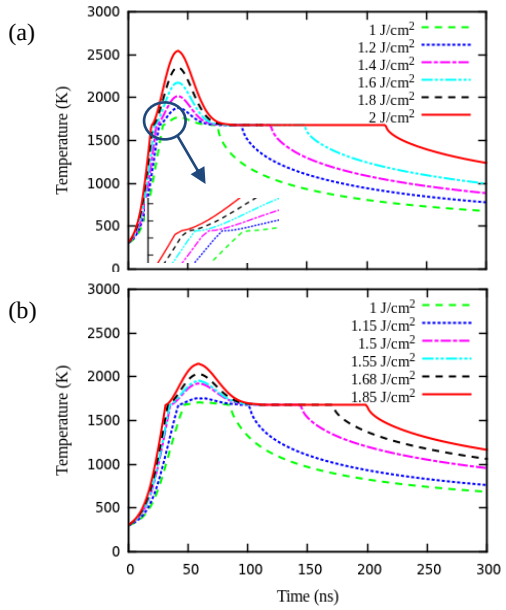

Figure 3. Temperature profile on the surface of the wafer as a function of time in the case of FWHM=32ns (a) and FWHM=45ns (b).

The results in figure 3 also demonstrate the effect phase transition on the time evolution of the temperature profile. As can be seen, the surface temperature increases rapidly from the initial temperature (i.e. 300K) to the Si melting point (i.e. 1683K). When the temperature rises above the melting point, a sharp decrease in the temperature rise rate is observed (enlarged section of figure 3(a)). This post-melting slows the heat transfer rate due to the enhanced surface reflectivity and the large absorption co-efficient of liquid Si. When the heat loss by conduction exceeds the energy gained by the laser radiation, the temperature decreases until the freezing point is reached. While the melting front (the position of the solid-liquid interface) sweeps back, the Si epitaxially recrystallises.

Figure 4 presents the melting front position as a function of time for different laser powers and the pulse durations of 32 ns and 45 ns. As can be seen, a higher laser power increases both the melting duration and the melting depth. However, the time of the maximum depths slightly increases when a higher laser power is used. Also, for a given laser power, a higher melting depth is observed for the pulse duration of 32 ns compared to that of 45 ns.

Figure 5 shows the melting front velocity as a function of time for different laser powers and pulse durations of 32 ns and 45ns. For both pulse durations, we found that the maximum re-crystallisation velocity is lower than the critical value for amorphisation of Si which is 15 m/s [22]. This indicates that, Si solidifies to a crystal rather than to an amorphous state. It can also be seen that, for a fixed pulse duration (such as 32 ns), the maximum re-crystallisation velocity is not a strong function of the laser power.

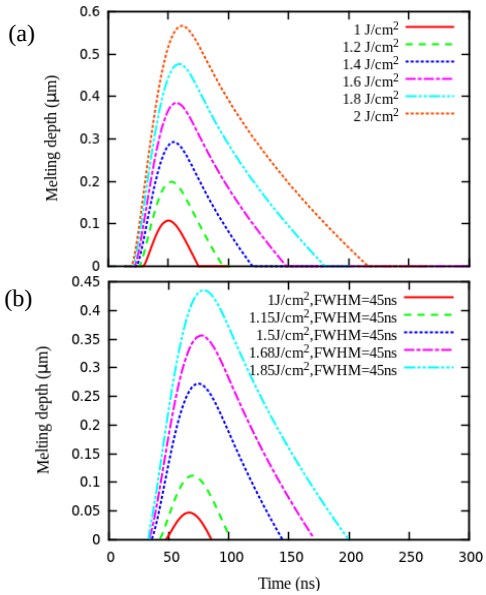

Figure 4. Melting depth evolution as a function of time in the case of FWHM=32ns (a) and FWHM=45ns (b).

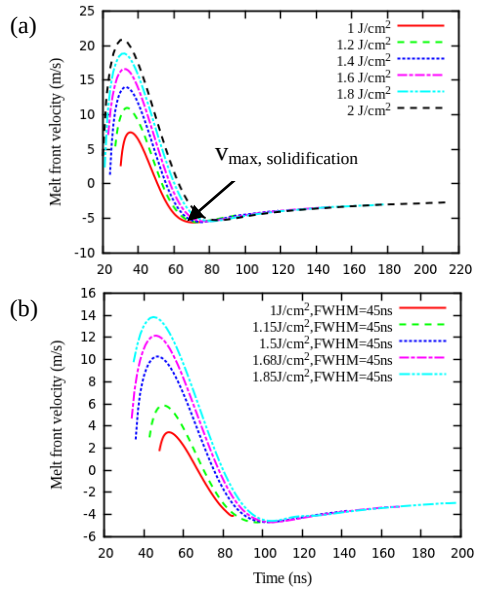

Figure 5. Melting front velocity as a function of time in the case of FWHM=32 ns (a) and FWHM= 45ns (b).

Figure 6 shows the non-dimensional melting depth and the melting front velocity as a function of time with the initial temperatures of 27°C, 300°C and 500°C. As can be seen, the melting duration increases with the increase of the initial temperature for the same amount of melting depth. On the other hand, re-crystallisation velocity decreases for a higher initial temperature.

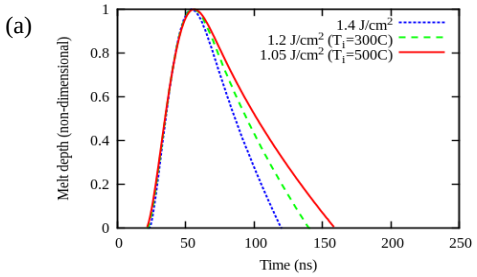

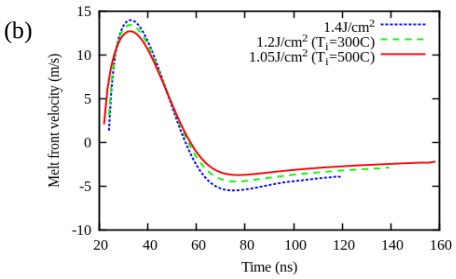

Figure 6. Non-dimensional melting depths (a) and melting front velocity (b) as a function of time with substrate temperatures of 27°C, 300°C and 500°C for the pulse duration of 32ns.

Also, introduction of the substrate heating relaxes the laser power density which may results in a reduction of the thermal gradients and hence thermal stress [4] within the wafer.

Conclusions

A numerical study of the nanosecond pulse laser induced melting and solidification of Si was presented in this paper. The implicit enthalpy method was employed to solve the transient heat conduction equation considering melting and solidification. A number of simulations were performed to study the effect of key parameters such as laser power, pulse duration and substrate initial temperature on the melting depth and duration, re-crystallisation velocity and maximum temperature. It was shown that a shorter pulse duration led to an increase in the melting depth. Also, for a given pulse duration, the maximum re-crystallisation velocity was almost independent of the laser power. Preheating of the wafer not only reduced the re-crystallisation velocity but also increased the melting duration. Our simulation results showed that for the laser power density in a range of 1 J/cm^2 to 2 J/cm^2, Si solidifies to a crystal rather than amorphous.

Acknowledgements

This work was supported by the Australian Research Council (ARC). The research benefited from computational resources provided through the National Computational Merit Allocation Scheme, supported by the Australian Government. The computational facilities supporting this project included the Australian NCI National Facility, the partner share of the NCI facility provided by Intersect Australia Pty Ltd., the Peak Computing Facility of the Victorian Life Sciences Computation Initiative (VLSCI), iVEC (Western Australia), and the UNSW Faculty of Engineering

References

[1] OpenCFD Ltd, 2014, http://www.openfoam.com.

[2] Hameri, Z., Mai, L., Puzzer, T., Sproul, A.B. & Wenham, S.R., Laser Induced Defects in Laser Doped Solar Cells, *Prog. Photovolt.*, 19(4), 2011, 391-405.

[3] White, C.W., Appleton, B.R., Christie, W.H., Pronko, P.P. & Wilson, S.R., Redistribution of Dopants in Ion Implanted Silicon by Pulsed Laser Annealing, *Appl. Phys. Lett.*, 33(7), 1978, 662-664.

[4] Wood, R.F. & Giles, G.E., Macroscopic Theory of Pulsed-Laser Annealing. I. Thermal Transport and Melting, *Phy. Rev.*, 23, 1981, 2923-2942.

[5] Fell, A. & Granek, F., Influence of Pulse Duration on the Doing Quality in Laser Chemical Processing (LCP)-A Simulative Approach, *Appl. Phys. A*, 110, 2013, 643-648.

[6] Lax, M., Temperature Rise Induced by a Laser Beam, *J. Appl. Phys.*, 48, 1977, 3919-3924.

[7] Lax, M., Temperature Rise Induced by a Laser Beam II. The Non-linear Case, *Appl. Phys. Lett.*, 33, 1978, 786-788.

[8] Moody, J.E. & Hendel, R.H., A general analytic technique for nonlinear dynamic transport processes during laser annealing, *J. Appl. Phys.*, 51, 1980, 3121-3125.

[9] Kim, M., Grosthwait, D.L. & Shah, R., A General Analytic Technique for Non-linear Dynamic Transport Processes During Laser Annealing, *J. Appl. Phys.*, 51, 1980, 3121-3125.

[10] Tokarev, V. & Kaplan, A.F.H., An Analytical Modelling of Time Dependent Pulsed Laser Melting, *J. Appl. Phys.*, 86, 2836-2846.

[11] Cole, J.M., Earwaker, L.G. & Humphreys, P., A Melting Model for Pulsed Laser Heating of Silicon, *Vac.*, 34, 1984, 871-874.

[12] Unamuno, S. De. & Fogarassy, E., A Thermal Description of the Melting of c- and a-Silicon Under Pulsed Excimer Lasers, *Appl. Surf. Sci.*, 36, 1989, 1-11.

[13] Aziz, M.J., Narayan, J., Stritzker, B. & White, C.W., Melting of Crystalline and Amorphous Silicon by Ruby, XeCl and KrF Laser Irradiation, *in: Proc. E-MRS*, 1985, 231-236.

[14] Hackenberg, M., Huet, K., Magna, A. La., Negru, R., Pichler, P., Pakfar, A., Tavernier, C. & Venturini, J., Enthalpy Based Modelling of Pulsed Excimer Laser Annealing for Process Simulation, *Appl. Surf. Sci.*, 258, 2012, 9347-9351.

[15] Fell, A., Kray, D. & Willeke,G.P., Transient 3D/2D simulation of laser-induced ablation of silicon, *Appl. Phys. A*, 92, 2008, 987-991.

[16] Schvan, P. & Thomas, R.E., Time-Dependent Heat Flow Calculation of CW Laser-Induced Melting of Silicon, *J. Appl. Phys.*, 57, 1984, 4736-4741.

[17] Poulain, G., Blane, D., Lemiti, M., Pellegrin, Y. & Semmache, B., Finite Element Simulation of Laser-Induced Diffusion in Silicon, *Ener. Proc.*, 8, 2011, 587-591.

[18] Li, Z., Ni, Xi., Shen, Z. & Zhang, H., Time-Resolved Temperature Measurement and Numerical Simulation of Millisecond Laser Irradiation Silicon, *J. Appl. Phys.*, 114, 2013, 033104:1-4.

[19] Azuma, H., Fukushima, H., Ito, T., Motohiro, T., Takeuchi, A., Takeuchi, A., & Yamaguchi, M., Pulsed KrF Excimer Laser Annealing of Silicon Solar Cell, *Sol. Ener. Mat. & Sol. Cells*, 74, 2002, 289-294.

[20] Voller, V.R., Fast Implicit Finite-Difference Method for the Analysis of Phase-Change Problems, *Numer. Heat Transfer B*, 17, 1990, 155-169.

[21] Minkowycz, W.J. & Sparrow, E.M., Computational Fluid Dynamics with Moving Boundaries, *Taylor & Francis*, 1996.

[22] Galvin, G.J., Mayer, J.W. & Peercy, P.S., Solidification Kinetics of Pulsed Laser Melted Si Based on Thermodynamic Consideration, *Appl. Phys. Lett.*, 46 (7), 1985, 644-646.